Optimization of elastic structures using boundary elements and a topological-shape sensitivity formulation

Rogério José Marczak
Mechanical Engineering Department, Federal University of Rio Grande do Sul, RS – Brazil

Abstract

The objective of this work is to present the implementation of topological derivative concepts in a standard BEM formulation. The topological derivative is evaluated at internal points, and those showing the lowest values are used to remove material by opening a circular cavity. Hence, as the iterative processes evolutes, the original domain has holes progressively punched out, until a given stop criteria is achieved. At this point, the optimal topology is expected. Several benchmarks of two-dimensional elasticity are presented and analyzed. Because the BEM does not employ domain meshes in linear cases, the resulting topologies are completely devoid of intermediary material densities. The results obtained showed good agreement with previous available solutions, and demanded comparatively low computational cost. The results prove that the formulation generates optimal topologies, eliminates some typical drawbacks of homogenization methods, and has potential to be extended to other classes of problems. More important, it opens an interesting field of investigation for integral equation methods, so far accomplished only within the finite element methods context.

1 Introduction

Topology optimization has been a major research subject in many engineering fields during the last decades, and a number of numerical methods has emerged to perform this type of computational design task efficiently. Among these, homogenization methods are possibly the most used approaches for topology optimization of structures. Since the early work of [1] these techniques and their variants have been successfully used in many structural optimization problems [2]. Because the technique deals with variable material densities, the finite element method (FEM) has became the natural choice for the numerical solution of the equations. Additionally, the technique is able to generate globally optimal solutions, i.e. microstrutured designs. Although strictly correct from the mathematical standpoint, this type of solution often fails to generate engineering designs in a straightforward manner. In order to render a 0-1 (void-material) solution, suboptimal microstructures with penalization like SIMP are used to avoid large areas with intermediate results (composite materials). Since the material distribution is related to the finite element mesh, results obtained through homogenization methods generally suffer

Mechanics of Solids in Brazil 2007, Marcílio Alves & H.S. da Costa Mattos (Editors)
Brazilian Society of Mechanical Sciences and Engineering, ISBN 978-85-85769-30-7

from mesh dependency. Another major drawback of the technique arises when some types of density gradient control are applied, possibly generating checkerboard instabilities that must be avoided in order to attain feasible designs. Another alternative method which has also been under development during the last years are the topological derivative (TD) or topological-shape sensitivity methods [3–5]. This family of methods aims the elimination of mesh dependency and numerical instabilities, two common drawbacks of homogenization methods.

Most of the research on topology optimization has been based on FEM methods (see, for instance, [6]). The objective of the present work is to apply a recently developed TD approach with boundary element methods (BEM). A previous methodology developed for heat transfer problems (Marczak, 2005) is extended to elasticity problems. Since the BEM does not need domain mesh, its use with TD methods renders a fully 0-1 approach, thus avoiding intermediary material densities and the associated numerical drawbacks. First, a review of the TD formulation adopted herein is addressed, which is particularized for 2D elasticity. Next, a numerical methodology is devised to carry out the computational design by an iterative BEM procedure. A number of examples are solved with the proposed formulation and the results are compared with available solutions.

2 A short review of topological-shape sensitivity for 2D elasticity equation

The idea behind topology derivative is the evaluation of a cost function sensitivity to the creation of a new cavity/hole. Wherever this sensibility is low enough the material can be progressively eliminated.

The original concept of topological derivative is related to the sensitivity of a given cost function ø when the topology of the analysis domain Ω is changed. The local value of the topological derivative at a point $\hat{\mathbf{x}}$ for this case evaluated by:

$$D_T^*(\hat{x}) = \lim_{\varepsilon \to 0} \frac{\psi(\Omega_\varepsilon) - \psi(\Omega)}{f(\varepsilon)} \tag{1}$$

where $\psi(\Omega)$ and $\psi(\Omega_\varepsilon)$ are the cost function evaluated for the original and the changed domain, respectively, and f is a regularizing, problem dependent, function. The major drawback of this concept is that it is not possible to establish an isomorphism between domains with different topologies, making the evaluation of Eq.(1) rather difficult or impossible.

Feijoo et. al [5] and Novotny et. al [7] circumvented this problem introducing the mathematical idea that the creation of a hole can be accomplished by simply perturbing an existing one, whose radius tends to zero (Fig. 1). Now both domains have the same topology and it is possible to establish a mapping between each other:

$$D_T(\hat{x}) = \lim_{\substack{\varepsilon \to 0 \\ \delta\varepsilon \to 0}} \frac{\psi(\Omega_{\varepsilon+\delta\varepsilon}) - \psi(\Omega)}{f(\varepsilon+\delta\varepsilon) - f(\varepsilon)} \tag{2}$$

where $\delta\varepsilon$ is a small perturbation on the hole's radius. It is important to note that Eq.(2) is formally rendering a shape sensitivity character to the original expression, but it can be proven that the Eqs.(1) and (2) are equivalent. The evaluation of D_T is, however, much easier than its original counterpart D_T^*.

In the present work, the interest rests on the evaluation of D_T for problems governed by the elasticity operator. Following the work of Novotny et. al [7], the topological derivative equations for linear elasticity will be reviewed. The direct problem is stated as:

$$\text{Find: } \{\mathbf{u}_\varepsilon \,|\mathrm{div}\sigma_\varepsilon = b\} \quad \text{on } \Omega_\varepsilon \tag{3a}$$

$$\text{Subjected to: } \begin{cases} \mathbf{u}_\varepsilon = \bar{\mathbf{u}} & \text{on } \Gamma_u \\ \sigma_\varepsilon \mathbf{n} = \bar{\mathbf{t}} & \text{on } \Gamma_t \\ \sigma_\varepsilon \mathbf{n} = 0 & \text{on } \Gamma_\varepsilon \end{cases} \tag{3b}$$

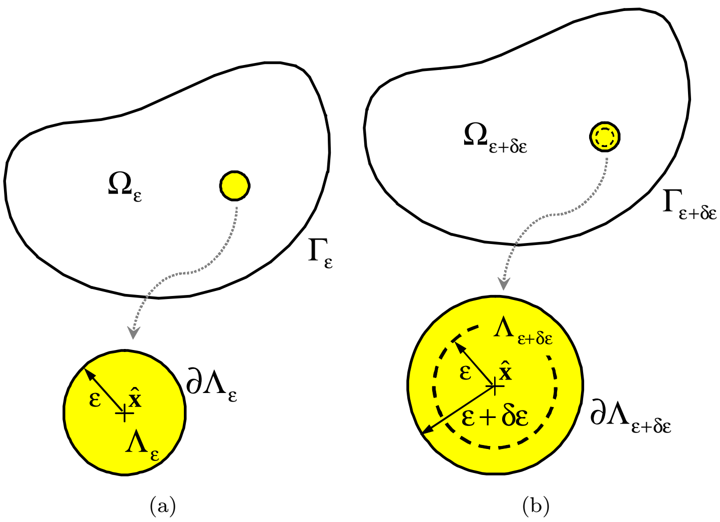

Figure 1: The modified concept of topological derivative. (a) Original domain. (b) Perturbed domain.

Let a general form for cost function be written as total strain energy function:

$$\begin{aligned} \Psi(\mathbf{u}_\tau) &= \frac{1}{2}\int_{\Omega_\tau} \mathbf{C}\nabla_\tau \mathbf{u}_\tau \cdot \nabla_\tau \mathbf{u}_\tau d\Omega_\tau - \int_{\Omega_\tau} \mathbf{b}\cdot \mathbf{u}_\tau d\Omega_\tau - \int_{\Gamma_t} \bar{\mathbf{q}}\cdot \mathbf{u}_\tau d\Gamma_\tau \\ &= \frac{1}{2} a_\tau(\mathbf{u}_\tau, \mathbf{u}_\tau) - l_\tau(\mathbf{u}_\tau) \end{aligned} \tag{4}$$

where τ is the perturbation parameter associated to the shape change velocity (i.e. $\mathbf{x}_\tau(\mathbf{x}) = x + \tau \mathbf{v}(\mathbf{x})$). The sensibility of the cost function with respect to τ can be obtained from the Gâteaux derivative

Mechanics of Solids in Brazil 2007, Marcílio Alves & H.S. da Costa Mattos (Editors)
Brazilian Society of Mechanical Sciences and Engineering, ISBN 978-85-85769-30-7

of the perturbed configuration given by Eq.(4):

$$\frac{d}{d\tau}\Psi\left(\Omega_\tau\right)_{\tau=0} = \lim_{\tau\to 0}\frac{\Psi\left(\Omega_\tau\right) - \Psi\left(\Omega_{\tau|\tau=0}\right)}{\tau} = 0 \;\text{ on } \partial\Gamma_\varepsilon \tag{5}$$

After an intensive analytical work, the topological derivative results, in absence of body loads:

$$D_T\left(\hat{\mathbf{x}}\right) = -\lim_{\varepsilon\to 0}\frac{1}{f'\left(\varepsilon\right)}\int_{\Gamma_\varepsilon}\frac{1}{2\rho E}\sigma_\varepsilon^{tt}d\Gamma_\varepsilon$$

Using an asymptotic analysis of the solution $\mathbf{u}_\varepsilon$, the following expression is found:

$$D_T\left(\hat{\mathbf{x}}\right) = \frac{2}{1+\nu}\sigma\cdot\varepsilon + \frac{3\nu-1}{2(1-\nu^2)}\mathrm{tr}\sigma\mathrm{tr}\varepsilon$$

which can be particularized for plane strain problems as

$$D_T\left(\hat{\mathbf{x}}\right) = \frac{2}{(1+\nu)(1-2\nu)}\sigma\cdot\varepsilon + \frac{(1-\nu)(4\nu-1)}{2(1-2\nu)}\mathrm{tr}\sigma\mathrm{tr}\varepsilon \tag{6}$$

A similar expression can be derived for the plane stress case.

3 Numerical methodology

In order to evaluate Eq.(6), the BEM was used in its direct version [8, 9]. Since the evaluation of physical variables on internal points with the BEM is a post-processing step, the recovery of local values for D_T can be easily implemented. Furthermore, because the BEM shows better accuracy for the evaluation of boundary variables than other popular methods like the FEM, it is expected a good performance of the approach for boundary points (which is an important issue in shape changes).

1. The optimization process is carried in four basic steps (see Fig. 2):
2. The standard BE problem is solved, and the variables are evaluated on a suitable grid of interior points.
3. The points with the lowest values of D_T are selected.
4. Holes are created by *punching out* disks of material centered on the previously selected points.
5. Check stopping criteria, rebuild the mesh, and return to step 1, if necessary.

At this point, the desired topology is expected. It is important to stress that, strictly speaking, the *punching* strategy here adopted is a type of *hard-kill* method for material elimination. This can be an issue in some non-convex problems, when material creation (filling) may occur simultaneously with material elimination.

It is worth to comment some aspects regarding the step 2. A common drawback in many shape and topology optimization methods is the progressive lost of symmetry in originally symmetric problems. This is related to the numerical evaluation of sensitivities, which are always prone to round-off and truncation errors. The material removal strategy also has influence on the final results, since symmetric topologies demand symmetric elimination of material. And of course the removal rate has a heavy

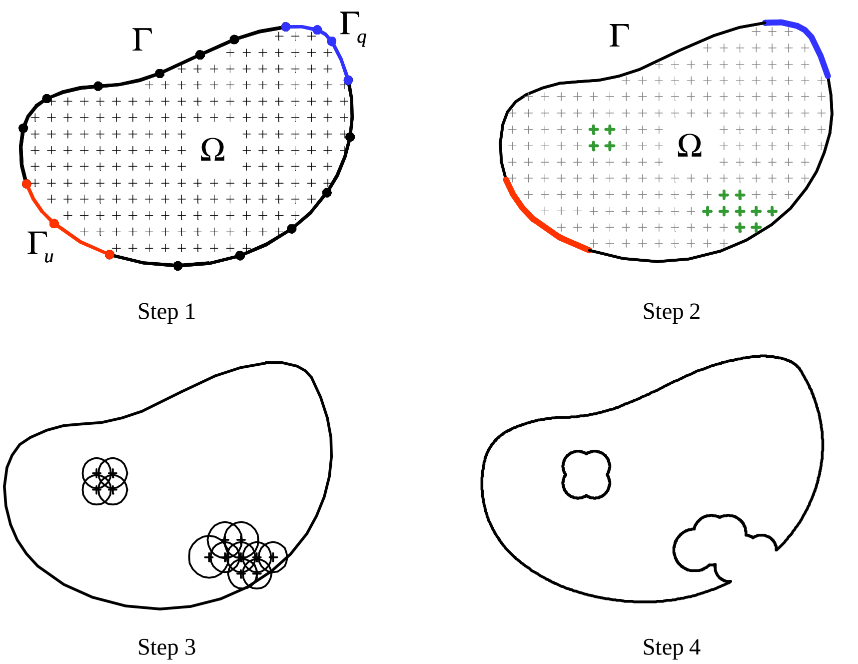

Figure 2: BEM iterative procedure for material removal.

influence on the computational cost of the analysis. These issues were faced in the early stages of the present work [10], and three strategies were successively devised to overcome it:

- **Method A**: Creation of a single hole per iteration: This is a very crude form of material removal, and computationally very inefficient. The point with the lowest D_T value is used to create the hole. Besides being unable to create more than one hole at each iteration (with obvious lost of symmetry), a large number of iterations is necessary to achieve a given solution.
- **Method B**: Creation of N_h holes per iteration: This is a natural improvement over method A, where a preset number of holes is allowed to be created at each iteration. It is computationally more efficient that its predecessor, but there is no simple way to guarantee symmetric solutions.
- **Method C**: It is a cut-off method: This method was devised to try to remove larger areas of material in each iteration. The ideal solution would be to remove all areas inside the isolines at a given level of topological derivative, for each iteration. A simpler shortcut is to define a cut-off value:

$$D_{\text{cutoff}} = \min\left(D_T^i\right) + \rho\left[\max\left(D_T^i\right) - \min\left(D_T^i\right)\right] \tag{7}$$

where i =1..number of sampling points (internal and boundary points). Therefore, all points with $D_T \leq D_{\text{cutoff}}$ are used to remove material.

After a number of preliminary tests, the methods B and C were found to be the best ones, and it was used throughout this work. By selecting suitable values of ρ, the rate of material removal can be controlled, provided it is not very large. Values in range $0.2\% \leq \rho \leq 5\%$ proved to be sufficient for most applications.

4 Numerical results

This section presents a number of cases analyzed using the proposed formulation. These are very preliminary results, used to test the formulation. Traction free boundary conditions were employed on the holes. In all cases, the total potential energy was used as the cost function. The total amount of material removed was checked at the end of each iteration and compared to a reference value until the desired volume is achieved. All cases used linear discontinuous boundary elements integrated with 8 Gauss points. The regularly spaced grid of internal points was generated automatically, taking into account the radius of the holes to be created during each iteration. The radius was taken as a fraction of a reference dimension of the domain ($r = \alpha l_{\text{ref}}$). They may vary in order to accelerate or decelerate the material removal rate, but usually $l_{\text{ref}} = \min(H, L)$ was adopted, where H and L are the height and length of the domain. The material volume is to be minimized in all cases. The current area of the domain (A_f) was checked at the end of each iteration until a reference value is achieved ($A_f = \beta A_0$, where A_0 is the initial value). The examples shown in this section employed circular holes discretized with six boundary elements.

4.1 Benchmark 1 - Fixed support

In this case a square domain has its left edge clamped and is subjected to a load on its upper right corner (Fig. 3). Holes with fixed radius were used throughout the process ($r = 0.025a$).

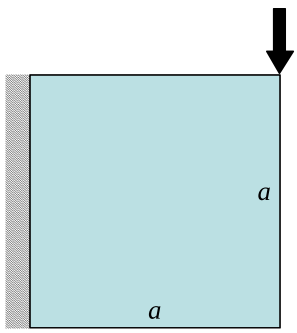

Figure 3: Illustration of benchmark 1.

The evolution history is shown in Fig. 4, for $N_h = 4$. The process was halted when $A_f = 0.4A_0$

was reached. Figure 5 shows the results obtained for this case when $N_h = 8$. Both cases delivered the same topologies, but evidently the solution was much faster in the latter one.

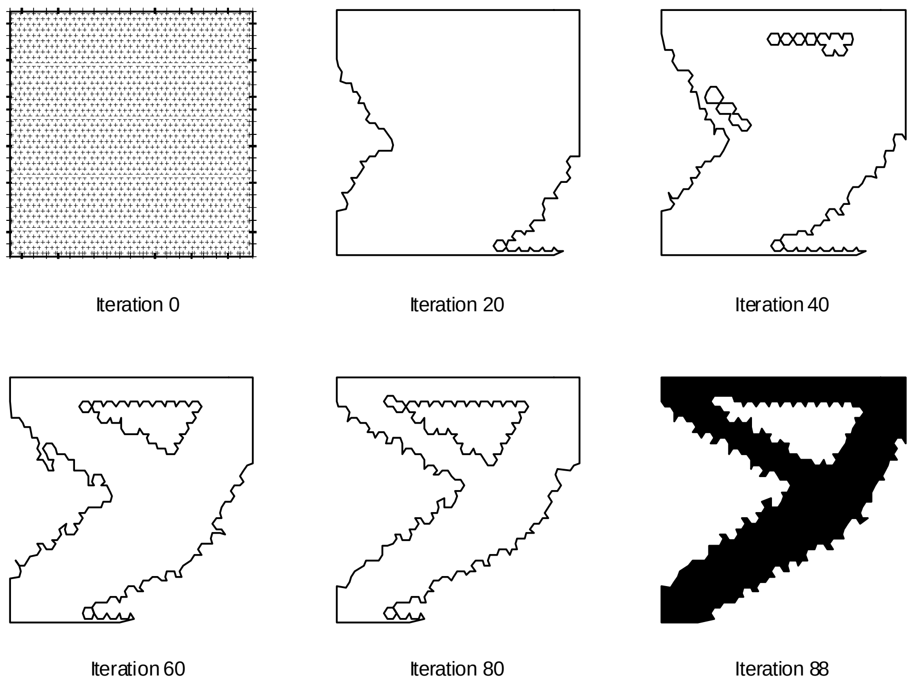

Figure 4: Optimization history of benchmark 1 – Method B with $N_h = 4$.

4.2 Benchmark 2 - Cantilever beam

In this case rectangular cantilever structure has its left edge clamped and is subjected to a load on its upper right corner (Fig. 6). Three different solution strategies were used to solve this problem.

The first solution used $r = 0.04a$ and method C with a fixed value of ρ in Eq.(7). The evolution history is shown in Fig. 7. Because a larger hole was used, the algorithm eliminated material very fastly, resulting a slender design with $A_f = 0.15A_0$ after 57 iterations.

The second solution used $r = 0.03a$ and method B with $N_h = 12$. As shown by the evolution history in Fig. 8, in this case the smaller radius of the holes and the more controlled material removal provided by method B allowed the formation of internal reinforcement bars, very similar to those also found in FEM homogenization solutions (Bendsøe 1995)(Bendsøe & Sigmund, 2003). The process was halted in the 40^{th} iteration, when $A_f = 0.35A_0$.

Mechanics of Solids in Brazil 2007, Marcílio Alves & H.S. da Costa Mattos (Editors)
Brazilian Society of Mechanical Sciences and Engineering, ISBN 978-85-85769-30-7

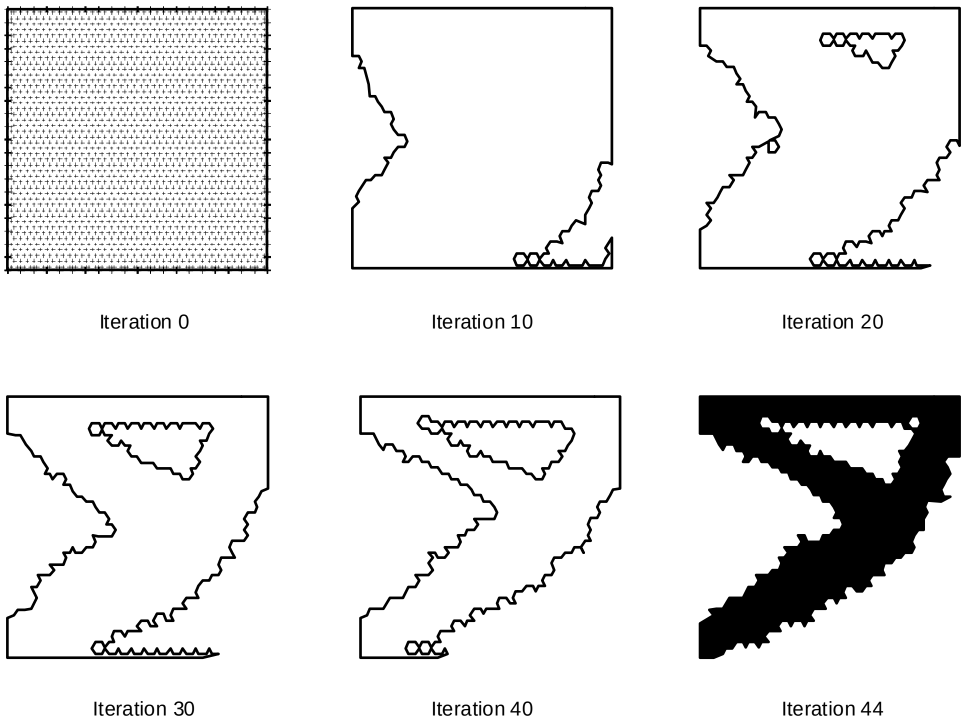

Figure 5: Optimization history of benchmark 1 – Method B with $N_h = 8$.

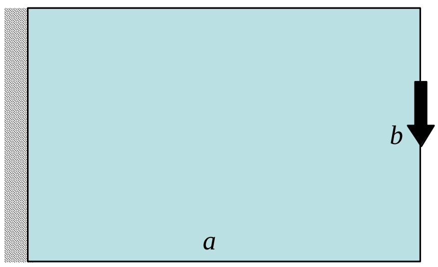

Figure 6: Illustration of benchmark 2.

The third solution repeated the last one, but using a slightly more dense internal points grid. As a consequence, the D_T sampling space was enriched and a more refined reinforcement pattern was found (Fig. 9).

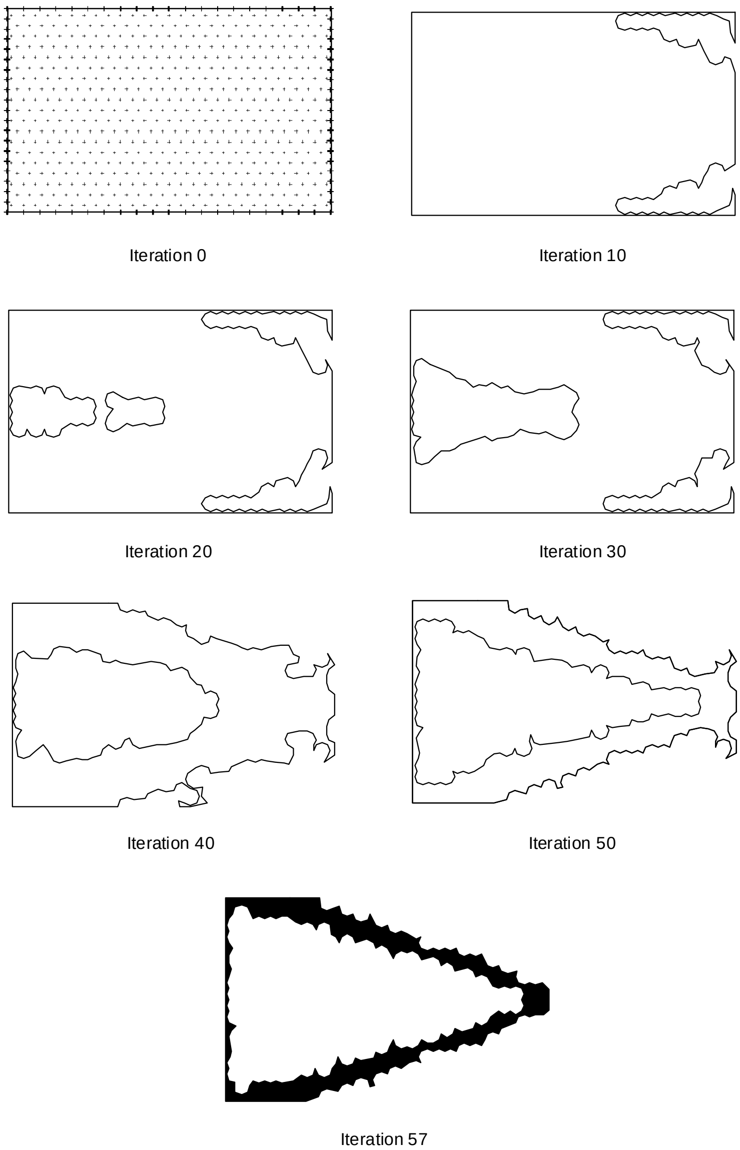

Figure 7: Optimization history of benchmark 2 - Method C with $r = 0.04a$.

The final design took 32 iterations to reach $A_f = 0.45A_0$. This dependence is deeply rooted in the existence of a global optimum, which is microstructured. As the internal mesh is refined (and the holes radius decreased) the likelihood of finding a microstructured solution also increases. This is in perfect agreement with similar results obtained with the FEM [11]. However, the BEM has the clear advantage of not dealing with intermediary material densities.

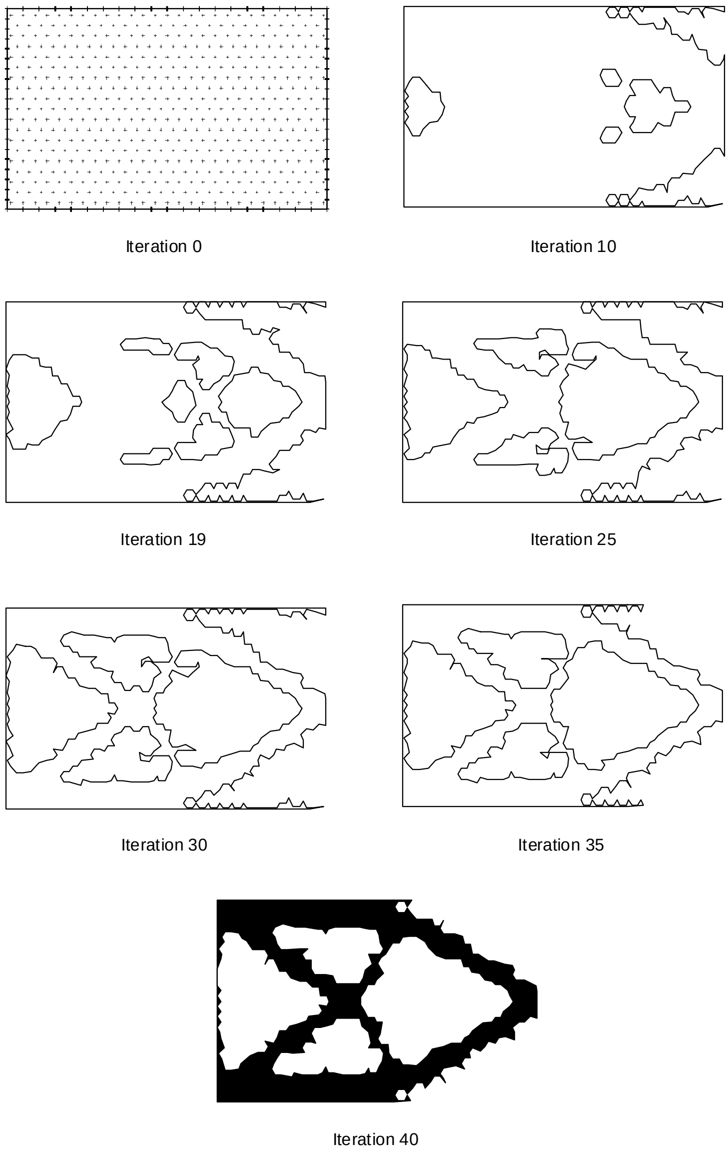

Figure 8: Optimization history of benchmark 2 - Method B with $r = 0.04a$ and $N_h = 12$.

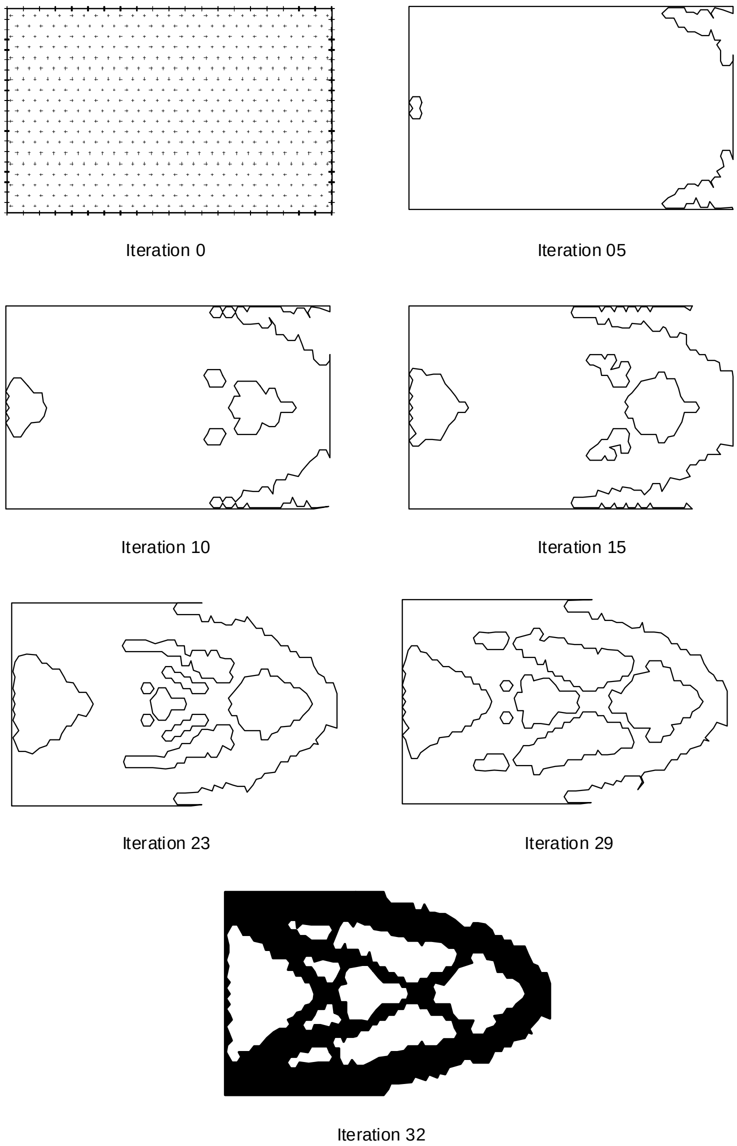

Figure 9: Optimization history of benchmark 2 - Method B with $r = 0.03a$ and $N_h = 12$.

4.3 Benchmark 3 - Michell truss

In this case refers to the popular Michell truss [12, 13]. The geometry, boundary conditions and loading for this benchmark are depicted in Fig. 10a. Two possible optimal solutions are shown in Fig. 10b.

The theoretical solutions of Fig. 10*b* have their configurations dependent on the number of bars used.

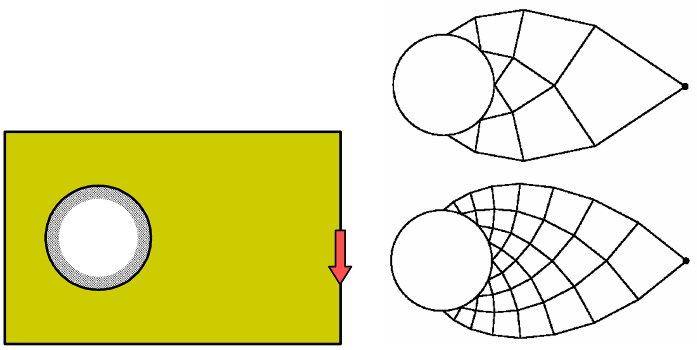

(a) (b)

Figure 10: (a) Illustration of benchmark 3. (b) Theoretical optimal solution (Michell truss).

This case was initially analyzed with the proposed formulation using method B with $r = 0.04a$ and $N_h = 2$. These parameters were found to be rather exaggerated to successfully generate a genuine Michell truss, as shown in the evolution history of Fig. 11, but the algorithm was able to detect their presence during intermediary iterations. This benchmark was reanalyzed using method B with $r = 0.02a$ and $N_h = 8$. The corresponding optimization history is depicted in Fig. 12. Here, the reinforcements are more clearly generated, resembling more closely the structure of Fig. 10*b*. Evidently, the use of smaller holes leads to a more representative design.

5 Conclusions

The present work introduced a topology optimization strategy for 2D elasticity problems using a topological derivative approach and the boundary element method. The relevant expressions for topological derivative evaluations are reviewed, aiming their implementation for problems governed by plane stress or plane strain equations. The formulation is derived by introducing a specially devised iterative material removal procedure in a BEM framework. Some classical benchmark cases are solved in order to verify the feasibility of the proposed procedure. Because the BEM does not employ domain meshes in linear cases, the resulting topologies are completely devoid of intermediary material densities. The obtained results showed good agreement with previous available solutions, and demanded comparatively low computational cost.

It is important to mention that the topological derivate approach presented herein is not a well posed problem from the optimization point of view. The cost function (potential energy density)

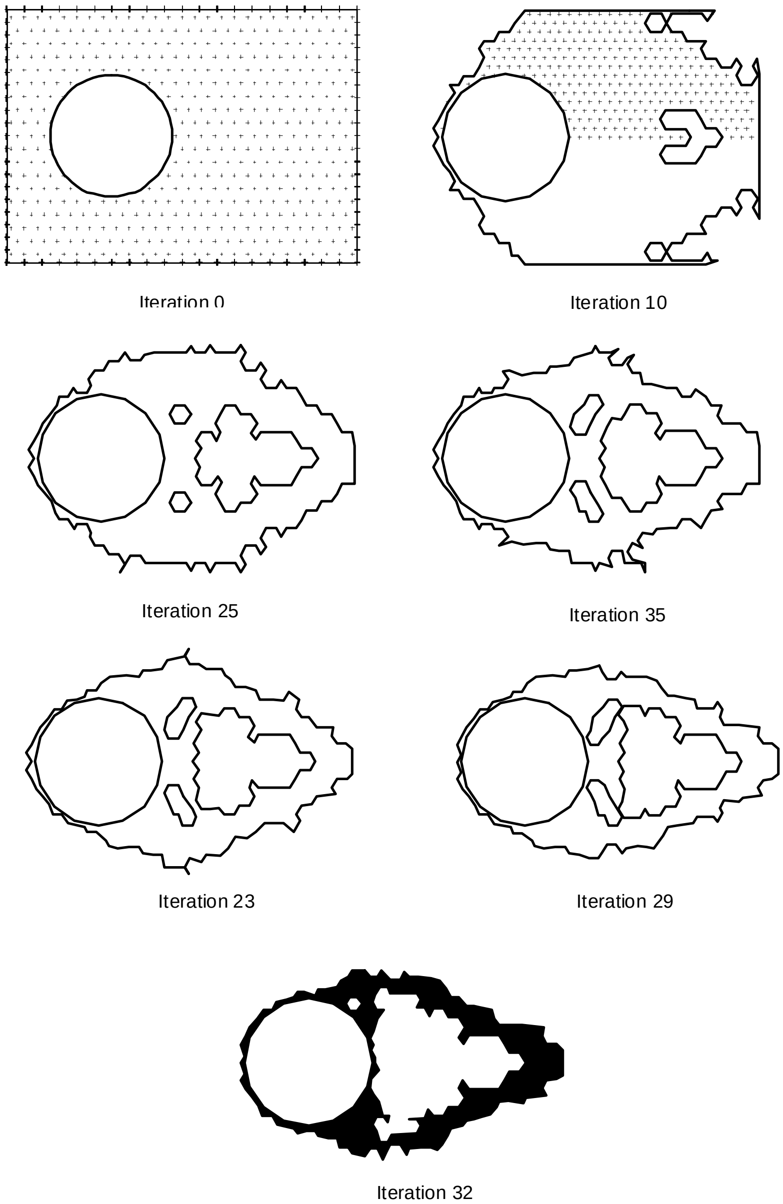

Figure 11: Optimization history of benchmark 3 - Method B with $r = 0.04a$ and $N_h = 2$.

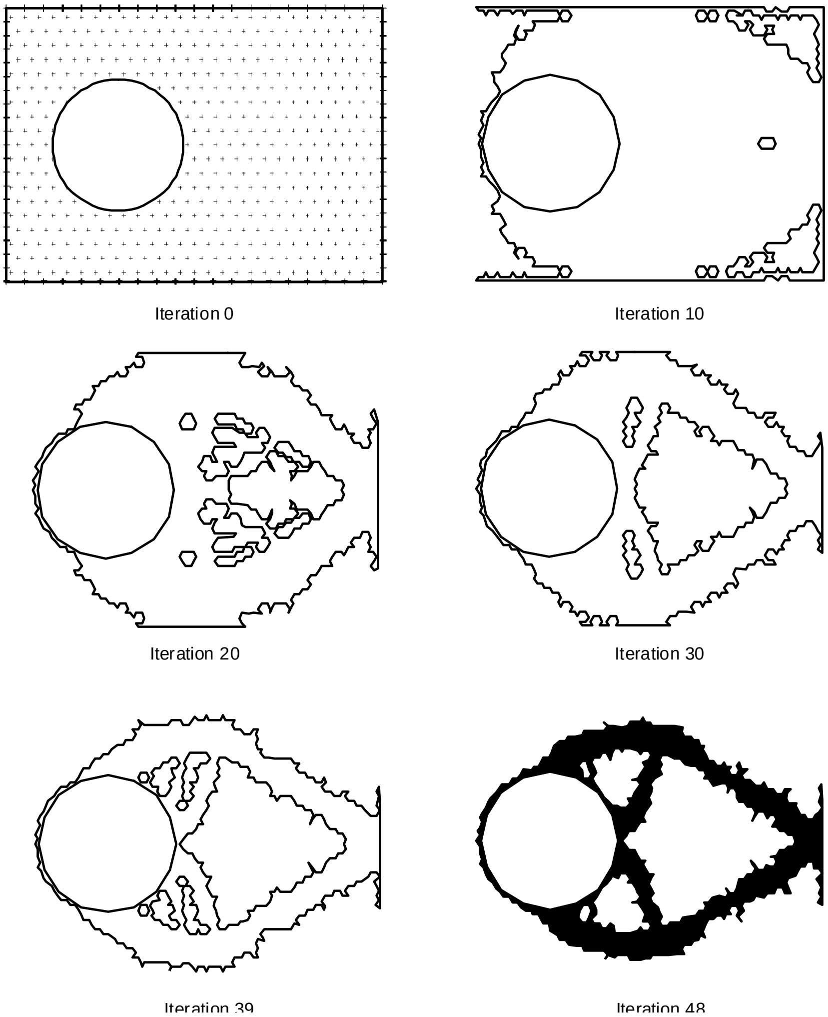

Figure 12: Optimization history of benchmark 3 - Method B with $r = 0.02a$ and $N_h = 8$.

is not explicitly given, and extensions of the formulation to other types cost function will demand elaborate analytical derivations. The imposition of constraints also deserves further investigation.

The presented results proved that the formulation generates optimal topologies, eliminates some typical drawbacks of homogenization methods, and has potential to be extended to other classes of problems like plates and 3D elasticity. The simplicity of the expressions used to estimate the sensitivities makes the extension of the method to other types of PDEs rather straightforward, the difference being only in the type of physical variables and sensitivities. More important, it opens an interesting field of investigation for integral equation methods, so far accomplished only within the finite element methods context.

References

[1] Bendsøe, M. & Kikuchi, N., Generating optimal topologies in structural design using a homogenization method. *Comput Methods Appl Mech Engrg*, **71**, pp. 197–224, 1988.

[2] Bendsøe, M. & Sigmund, O., *Topology Optimization. Theory, Methods, and Applications*. Springer-Verlag, 2003.

[3] Sokołowski, J. & Żochowski, A., On topological derivative in shape optimization. Technical report, INRIA-Lorraine, France, 1997.

[4] Sokołowski, J. & Żochowski, A., Topological derivatives of shape functionals for elasticity systems. *Mech Struct Mach*, **29**, pp. 331–349, 2001.

[5] Feijoo, R., Novotny, A., Padra, C. & Taroco, E., The topological-shape sensitivity analysis and its applications in optimal design. *Mecanica Computacional*, eds. S. Idelsohn, V. Sonzogni & A. Cardona, Santa Fe-Parana - Argentina, volume XXI, 2002.

[6] Mackerle, J., Topology and shape optimization of structures using fem and bem - a bibliography (1999–2001). *Finite Elements in Analysis and Design*, **39**, pp. 243–253, 2003.

[7] Novotny, A., Feijoo, R., Taroco, E. & Padra, C., Topological-shape sensitivity analysis. *Comput Methods Appl Mech Engrg*, **192**, pp. 803–829, 2003.

[8] Brebbia, C., Telles, J. & Wrobel, L., *Boundary Element Techniques - Theory and Applications in Engineering*. Springer-Verlag: Heildelgerg, 1984.

[9] Brebbia, C. & Dominguez, J., *Boundary Elements - An Introductory Course*. Computational Mechanics Publications, 1989.

[10] Marczak, R., (ed.), *Topology optimization and boundary elements - a preliminary implementation for linear heat transfer*, Brazilian Assoc. for Comp. Mechanics & Latin American Assoc. of Comp. Methods in Engineering, XXVI Iberian Latin-American Congress on Computational Methods in Engineering - CILAMCE 2005: Guarapari-Espírito Santo - Brazil, 2005.

[11] Sigmund, O. & Petersson, J., Numerical instabilities in topology optimization: A survey on procedures dealing with checkerboards, mesh dependencies and local minima. *Structural Optimization*, **16**, pp. 68–75, 1998.

[12] Michell, A., The limits of economy in frame structures. *Phil Mag*, **8**, pp. 589–597, 1904.

[13] Ostoja-Starzewskiy, M., (ed.), *Michell trusses in the presence of microscale material randomness: limitation of optimality*, volume A-457, R. Soc. Lond., 2001.